A heterodyne Phase Contrast Imaging system for Ion Cyclotron Emission detection

A. Marinoni,[1, a)] C.P. Moeller,[2] J.C. Rost,[1] M. Porkolab,[1] and E.M. Edlund[1, b)]
[1)]*Plasma Science and Fusion Center, Massachusetts Institute of Technology, Cambridge (MA) 02139, USA*
[2)]*General Atomics, San Diego (CA) 92121, USA*

(Dated: 28 June 2020)

The Phase Contrast Imaging diagnostic on the DIII-D tokamak has been upgraded with a novel optical heterodyne detection scheme to detect electron density fluctuations at frequencies of tens of megahertz. The novel system can be employed to measure the radial structure of the electron density component of Ion Cyclotron Emission (ICE), thus extending the purely temporal measurements provided so far by magnetic probes. The heterodyne system considerably extends the frequency response of the PCI method by modulating the probing laser beam at a frequency close to that of the wave of interest, thus placing the detected beat wave within the frequency bandwidth of the detector array. The system employs ~~an~~ a variable frequency Electro-Optic modulator to allow operation at any frequency in the range 5–50 MHz, where most of the ICE harmonics are observed on DIII-D. The use of an EOM allows one to operate the system at various frequencies without the need to realign the system. The response of the EOM to the modulation frequency and the driving voltage is reported.

I. INTRODUCTION

Waves in magnetically confined plasmas is a broad and complex topic that has been the subject of intense theoretical and experimental investigations for nearly a century. Its extent can be appreciated by noting that oscillations span several orders of magnitude both in frequency, from kHz to hundreds of GHz, and spatial scales, from the electron gyro-radius to the size of the plasma itself, either as turbulent or coherent phenomena. The experimental characterization of the entire spectrum of waves is an extremely challenging task due to constraints in the measurements; such limitations can be of a technological nature, e.g. inadequate signal to noise ratio or spatio-temporal response of the apparatus in use, or due to the inability to detect a given component of the wave under consideration. In this work we expose a method to detect the spatio-temporal characteristics of a particular class of instabilities in the cyclotron range of frequencies, commonly referred to Ion Cyclotron Emission (ICE). First predicted in the 1950s[1–4], this class of waves is believed to be a Compressional Alfvén Eigenmode generated by anisotropies, or inversions, in the distribution function of energetic particles that causes emission of electromagnetic radiation in bands centered around the thermal ion cyclotron frequency, as well as higher harmonics[5]. While ICE was first observed in the late 1970s on the TFR tokamak[6], it sparked increasing interest in the fusion community only from the early 1990s thanks to its suitability as a passive diagnostic tool of the energetic ion population that is compatible with the harsh environment in future fusion reactors. As such, it was searched for and observed on many magnetically confined plasma devices[7–17] which detected emission caused by either supra thermal beam ions or fusion products. Although there exist numerous measurements of frequency spectra and toroidal mode numbers on various plasma discharge actuators, the radial and poloidal structure of the instability are still elusive because all the reported measurements were performed using either external magnetic loops or heating antennas operated in receiving mode, both of which are not capable of directly measuring the RF field components in the plasma core. More specifically, diagnostic systems that are usually employed to detect the radial or poloidal structure of a given instability cannot detect ICE because its frequency exceeds the diagnostic bandwidth. The system described in this work was conceived to fill such gap and provide further constraints to the theoretical description of the instability which is not yet complete, especially in the non-linear phase[18].

The paper is organized as follows: Section II gives an overview of the Phase Contrast Imaging method; the technical details of the heterodyne PCI for ICE detection are described in Section III; conclusions are offered at the end.

II. THE PHASE CONTRAST IMAGING METHOD

The Phase Contrast Imaging (PCI) method is an optical technique that uses probing light traveling through a transparent medium, and converts phase shifts induced on the probing wavefront into amplitude variations at the image plane. Invented in the 1930s by F. Zernike[19], who proved its superior sensitivity compared to competing methods used in cellular microscopy, its application to plasmas was pioneered by M. Presby and D. Finkelstein in the late 1960s[20] and its application to measure the dispersion of waves in fusion grade plasmas may be attributed to H. Weisen in that late 1980s[21]. In very simplistic terms, the

[a)]marinoni@mit.edu
[b)]Present address: SUNY Cortland, Cortland (NY) 13045, USA

PCI technique can be described as an internal reference interferometer, i.e. for which both legs travel through the plasma, that measures the spatial distribution of electron density fluctuations by imaging the probing laser beam onto an array of detectors. More specifically, for fluctuations with wavelengths of a few mm to a few cm, which are typically active in modern fusion devices, and at the probing wavelength of 10.6 μm, which is commonly used by PCI systems worldwide, diffraction occurs in the Raman-Nath rather than in the Bragg regime. In such conditions, the plasma behaves as a transparent object in which phase shifts caused by the plasma are small, usually below milli-radiant levels, and are given by

$$\varphi(\mathbf{x}_\perp, t) = \lambda_0 r_e \int_a^b dx_\parallel \, n_e(\mathbf{x}, t), \qquad (1)$$

where λ_0 is the wavelength of the probing laser beam in vacuum, r_e is the classical electron radius, n_e is the plasma electron density and the parallel spatial coordinate refers to the propagation direction of the probing laser beam. The total phase shift, φ, is usually decomposed into a component given by the stationary plasma density, $\varphi_0(\mathbf{x}_\perp)$, and that due to fluctuations, $\tilde{\varphi}(\mathbf{x}_\perp, t)$, which is usually much smaller than the former. The technique relies on the $\pi/2$ phase shift between the two legs of the interferometer, as expressed in the following Maclaurin first order expansion of the total electric field, E_{tot}, of the probing wave

$$E_{tot}(\mathbf{x}_\perp, t) = E_0 e^{\imath\varphi(\mathbf{x}_\perp, t)} \approx E_{\varphi_0}[1 + \imath\tilde{\varphi}(\mathbf{x}, t)], \qquad (2)$$

where spatial dependencies of the stationary plasma density and of the probing electric field have been omitted for simplicity. Equation 2 states that the total electric field, E_{tot}, is composed of the reference leg field that has interacted with the stationary plasma density, E_{φ_0}, plus that of the measurement leg that has interacted with the fluctuating plasma density, $E_{\varphi_0}\imath\tilde{\varphi}$. The PCI method employs the scattering angles at which the measurement and the reference beams propagates with respect to each other, and separates these two components in a suitable focal plane of the imaging system, where an additional $\pi/2$ phase shift is induced. Additionally, in oder to increase the contrast between the two components, the intensity of the reference beam is usually attenuated by a factor $\rho < 1$. The *invisible* phase shifts are thereby made *detectable* as variations in brightness, I, according to the relation

$$I(\mathbf{x}_\perp, t) \approx I_{\varphi_0}\rho \left(1 \pm \frac{2}{\rho}\tilde{\varphi}(\mathbf{x}_\perp, t)\right). \qquad (3)$$

Equation 3 shows that the sensitivity of a PCI system is a factor $2/\rho$ that of a comparable standard homodyne interferometer operated in optimal detection mode (i.e. with the two legs exactly out of phase), with other parameters being equal.

A. Heterodyning PCI methods

The PCI method is particularly attractive in the field of experimental plasma turbulence because it images fluctuations onto an array of linear detectors, thereby making the extraction of spatio-temporal spectra feasible. However, due to technological limitations in manufacturing arrays of cryo-genically cooled detectors used to image the plasma, worldwide PCI systems typically use Photo-Conductive or Photo-Voltaic detectors whose 3dB points are within 1 MHz and 10 MHz, respectively. Although suitable for broadband turbulence and low frequency waves, such narrow bandwidths preclude the study of faster phenomena, whose detection requires the use of suitable heterodyning techniques. By modulating the intensity of the probing laser beam at a frequency close to that of the wave of interest the heterodyne beat frequency falls within the PCI detector bandwidth, thus making the imaging method applicable at higher frequencies. Such technique has recently been used on the Alcator C-Mod tokamak to detect Ion Cyclotron waves which discovered the mode converted ion cyclotron slow waves (ICW)[22], and by employing the absolute calibration of the PCI system, yielded the first quantitative experimental validation of full-wave models[23]. On the heterodyne PCI system installed on Alcator C-Mod, modulation of the intensity of the laser beam was obtained using Acousto- Optic Modulators (AOMs), which consist of a crystal in which a piezoelectric transducer, driven by an appropri- ate electric field, excites the propagation of an acoustic wave. The crystal then behaves as a time varying, periodic, diffraction grating which scatters incoming light at the Bragg angle and shifts it in frequency by that of the sound wave. The required intensity modulation of the incoming light is obtained by subsequently recombining the scattered and unscattered components. This method, although successfully used on Alcator C-Mod, would not be the preferred solution in our case due to the fact that AOMs typically operate within a narrow bandwidth, of the order of a few MHz, around the frequency of the acoustic wave which, additionally, can only be chosen among a finite set of values (typically multiples of 40 MHz for incident light of 10.6 MHz wavelength). As such, the overall modulation frequency can only be varied by ~~opportunely~~ combining multiple AOMs, which results into a number of disadvantages hereafter described. Firstly, the modulation frequency cannot be chosen at will but is a linear combination of the modulation frequencies of each AOM. Secondly, the system complexity and the real estate occupied on the optics table rapidly increase with the number of AOMs used. Thirdly, the system has to be realigned every time the modulation frequency is altered. These constraints are in direct conflict with our detection requirements because ICE is typically observed over several harmonics spaced by the cyclotron frequency which, on DIII-D, additionally, can be continuously modified in the range 6–15 MHz by varying the confining magnetic field. In view of the above, it is apparent how the ability to modify the modulation frequency of the heterodyne

system is of paramount importance to ICE detection. It was therefore decided to employ an Electro-Optic modulator (EOM) to overcome the aforementioned shortcomings of the AOMs. Indeed, since EOMs offer continuously variable modulation from DC to GHz bandwidth without altering the beam path of the probing light, the PCI system can be used in heterodyne mode at any available frequency; standard homodyne operation mode for broadband turbulence detection is recovered simply by turning off the EOM driver.

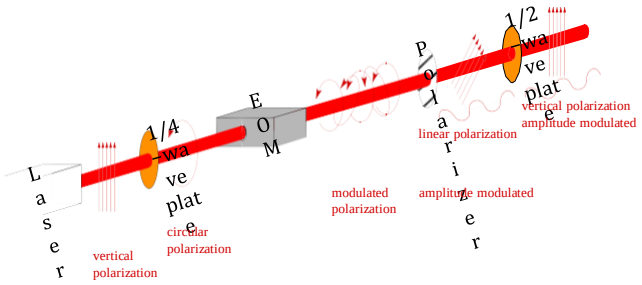

FIG. 1. Conceptual layout of a beam polarization preserving EOM.

III. TECHNICAL IMPLEMENTATION

A. Pockels cell

The typical set-up of an EOM consists of a Pockels cell located between two crossed polarizers, i.e. oriented at 90 degrees with respect to each other; the second polarizer achieves the amplitude modulation by projecting along a fixed axis the time varying polarization induced by the Pockels cell. For light at 10.6 μm it is necessary to use birefringent crystals that belong to the symmetry group $\bar{4}3m$, for which the magnitude of the electro-optic coefficient is such that Pockels cells must be used in a transverse configuration. In such case, the time varying intensity of the probing light electric field at the exit of the modulator reads[24]

$$I_{out}(t) = I_0 \sin[k_0 n_0^3 r_{41} E_{ext}(t) L/2]^2 \qquad (4)$$

where I_0 is the intensity of the probing light, I_{out} that of the light exiting the EOM, L the crystal length along the propagation direction of the probing light, k_0 the probing beam vacuum wave vector, n_0 the vacuum index of refraction of the crystal at the wavelength of the probing light, E_{ext} the time varying electric field externally applied to the birefringent crystal and r_{41} the electro-optic coefficient of the crystal. It is apparent from ~~equation~~ Eq. 4 that, in order to obtain an on-off modulation, the argument of the sinusoidal function, which is the phase shift between the ordinary and the extraordinary components of the probing light polarization, has to be close to $\pi/2$. The actual set-up used in this work is depicted in Fig. ~~figure~~ 1, from which it can be noted that the first polarizer is absent and that a quarter- and half-wave wave-plates are located before the Pockels cell and after the exit polarizer, respectively. While the absence of the entry polarizer is justified by the fact that the probing laser is already linearly polarized along the appropriate direction, the wave- plates are used to make the overall intensity modulation linearly proportional to the sinus of the external electric field. Indeed, by applying a quarter-wave difference be- tween the ordinary and extraordinary components of the probing light Eq. ~~equation~~ 4 becomes

$$I_{out}(t) = I_0 \sin[\delta + \pi/4]^2 = I_0 \frac{1+\sin(2\delta)}{2} \qquad (5)$$

shift. The half-wave plate after the exit polarizer is used to rotate the laser polarization to the original direction to preserve correct functioning of other components in the optical system.

The birefringent crystal is shaped as a regular parallelepiped with dimensions 5x5 mm^2 and 5 cm, respec- tively, across and along the propagation direction of the laser beam. The crystal dimensions were chosen in such a way as to maximize the phase shift δ, viz. length- ening the crystal at fixed applied voltage, while main- taining the cross section large enough for the crystal not to become structurally too fragile. Overall, the cross- sectional dimension is a compromise between the need to accommodate a collimated laser beam while not re- quiring too large of a voltage for a given external electric field intensity, which is one of the quantities determin- ing the overall modulation depth via the phase shift δ. Finally, cost considerations apply to the total volume of the crystal. The crystal is water cooled for thermal sta- bility and cut along the Miller indices that maximize the phase shift δ, other quantities being equal. More specifi- cally, the cross section is oriented along directions $(\bar{1}10)$, gold coated electrodes are applied on the surface (110), while the water cooled surfaces are in contact with sur- face (001). The crystal was chosen to be CdTe because, among birefrengent materials suited for light at 10.6 μm wavelentgh, it features the largest electro-optic coefficient thereby lowering the voltage requirements for a given crystal size. More specifically, for the case of the crystal and the optical set-up used in this work, 100% modula- tion depth is theoretically obtained with sinusoidal am- plitude of 2217 V, as opposed to 3410 V for ZnTe, 4926 V for GaAs and 8867 V for ZnSe. The actual behavior of Pockels cell is not exactly that described by equation 5 which, instead, models the adiabatic approximation, i.e. the limit in which light travel time along the crystal is negligible compared to the modulation frequency. In real- ity, the transit time has to be accounted for which reduces the phase delay δ by the quantity $\rho = |\sin(\pi f\tau)/(\pi f\tau)|$, where f the modulation frequency and τ the time re- quired by photons to travel through the crystal[25]. for the system in use the attenuating factor ρ is equal to

about 99.9%. In a purely capacitive component such as a Pockels cell, dielectric losses are the primary cause of

where δ is defined as half of the afore-mentioned phase

power dissipation in the system and, therefore, determine

the minimum power to be removed by the cooling system and provided by the RF driver. In the case of a dielectric subject to a sinusoidal electric field, it can be shown[22] that the power per unit volume dissipated in the dielectric is equal to

$$\frac{dP_{loss}}{dV} = \frac{1}{2}\omega\,\varepsilon_d(\omega)\tan(\theta)\,|E_{ext}|^2\,, \qquad (6)$$

where ω is the modulation angular frequency, ε_d is the real part of the permittivity and $\tan(\theta)$ is a parameter known as *loss tangent*. Detailed measurements of the loss tangent for CdTe are not readily available in the literature; however, interpolation over existing data indicates that, for the ICE frequency range, dielectric losses should not exceed 1 W, thereby making heat removal not problematic.

B. Voltage driver

Before describing how the voltage driver has been designed an built, it is useful to state the actual response of the Pockels cell based on the time evolution of the externally applied voltage. In the optical set-up described by equation 5, the intensity modulation produced by a crystal of size d subject to a voltage amplitude V_0 oscillating at frequency ω, is a sinusoidal function of the phase shift which, in turn, is linear in the applied voltage; as a consequence, a sinusoidally varying electric field generates higher order harmonics in the intensity modulation. Indeed, the Jacobi-Anger equation

$$e^{\imath z\cos\theta} = \sum_{n=-\infty}^{\infty} \imath^n J_n(z) e^{\imath n\theta} \qquad (7)$$

together with Euler's formula, can be used to compute the harmonic expansion of Eq. ~~equation~~ 5 to yield

$$\sin[z\cos(\theta)] \equiv \frac{e^{\imath z\cos(\theta)} - e^{-\imath z\cos(\theta)}}{2\imath} = \sum_{n=-\infty}^{\infty} \imath^{2n} J_{2n+1}(z) e^{\imath(2n+1)\theta}\,, \qquad (8)$$

which shows that the strength of the n-th harmonic is the n-th order Bessel function of the first kind, and that even harmonics do not contribute to the signal (in our case $z \propto V_0$ and $\theta \equiv \omega t$). The argument of the Bessel function, z, is the maximum phase shift between the ordinary and the extraordinary components of the laser beam which is between zero and $\pi/2$, respectively corresponding to 0% and 100% modulation depths. By imposing that the amplitude of the first spurious component, i.e. that at three times the fundamental frequency, in the intensity of the modulated beam be at most one-hundredth of that at the fundamental frequency, one obtains that the modulation depth cannot exceed 50%, or one-third

FIG. 2. Reduced diagram of the variable frequency high voltage oscillator.

FIG. 3. Modulation depth of the EOM as a function of the modulation frequency.

the modulation depth, and are therefore not expected to significantly bias the heterodyne detection scheme. The presence of third and higher order harmonics represents an appreciable issue for the detection of fluctuations over extended bandwidth, such as ICE, because the higher harmonics might happen to beat with actual waves oscillating at similar frequency, thereby producing a low-frequency signal within the detector bandwidth that could bias the analysis. In case a 100% modulation depth was required, e.g. for S/N considerations, one remedy to the higher order harmonics would be to modulate the voltage with a triangular waveform, so that an almost pure sinusoidal intensity modulation would be obtained. However, such scheme would cause spectral contamination at odd harmonics when the modulation depth was not close to 100%.

In view of the considerations above, the voltage driver was designed to deliver a sinusoidal waveform of 1 kV amplitude, plus XXX% set as contingency in case enhanced modulation depth will ever e needed. The principle of operation is that of a tank circuit which resonates in an extended frequency range thanks to two variable capacitors. It operates according to a feed-back loop where the frequency set by the resonator is sampled and amplified by JFET transistors assembled in a crossed coupled capacitors configuration. The circuitry is shown in Fig. ~~figure~~ 2

IV. SYSTEM RESPONSE

the quarter-wave voltage. Higher components are well below one-thousandth for almost all possible values of

The response of the complete system composed of the CO_2 laser, wave-plates, Pockels cell, high voltage driver was tested on an optical table to characterize the re- sponse as a function of the modulation frequency. The frequency response of the entire EOM is displayed in Fig. ~~figure~~ 3, while the response to the applied voltage to the crystal is found in Fig. ~~figure~~ 4. The transmissivity of the Pockels cell with no applied voltage was measured to be 98%.

FIG. 4. Modulation depth of the EOM as a function of the voltage applied to the crystal for a modulation frequency equal to ZZZ MHz.

V. CONCLUSIONS

This work describes the design and realization of a heterodyne Phase Contrast Imaging system to detect Ion Cyclotron Emission waves in tokamaks. The system is designed to be employed on the existing PCI diagnostic on DIII-D by modulating the intensity of an infrared laser beam at 10.6 ␮m wavelength and in a broad frequency region. The modulator is made of a water cooled CdTe Pockels cell driven by a resonant circuit able to generate sinusoidal waveforms up to 2 kV pk-pk, which guarantees adequate detection bandwidth. The circuit is able to drive the cell at any frequency in the region 5–50 MHz, thanks to a continuously variable frequency oscillator. The modulation depth is measured to be equal to XXX with a flat frequency response within YYY %.

ACKNOWLEDGMENTS

This work was supported by the US Department of Energy under DE-FG02-94ER54235. Data shown in this paper can be obtained in digital format by following the links at https : //fusion.gat.com/global/D3D DMP.

[1]K. G. Malmfors, Arkiv Fysik **1**, 569 (1950).

[2]E. P. Gross, "Plasma oscillations in a static magnetic field," Phys. Rev. **82**, 232–242 (1951).

[3]H. K. Sen, "Solar "enhanced radiation" and plasma oscillations," Phys. Rev. **88**, 816–822 (1952).

[4]E. G. Harris, "Unstable plasma oscillations in a magnetic field," Phys. Rev. Lett. **2**, 34–36 (1959).

[5]R. Dendy, C. Lashmore-Davies, and K. Kam, "A possible excitation mechanism for observed superthermal ion cyclotron emission from tokamak plasmas," Physics of Fluids B: Plasma Physics **4**, 3996–4006 (1992).

[6]Equipe-TFR, "High-power neutral injection and ion power balance in TFR," Nuclear Fusion **18**, 1271–1303 (1978).

[7]S. Yamamoto, K. Itoh, A. Fukuyama, and S. Itoh, "Plasma heating by multiple-short-pulse neutral beams," Plasma Physics and Controlled Nuclear Fusion Research **1**, 665 (1984).

[8]G. Cottrell, V. Bhatnagar, O. D. Costa, R. Dendy, J. Jacquinot, K. McClements, D. McCune, M. Nave, P. Smeulders, and D. Start, "Ion cyclotron emission measurements during JET deuterium-tritium experiments," Nuclear Fusion **33**, 1365–1387 (1993).

[9]H. Duong, W. Heidbrink, E. Strait, T. Petrie, R. Lee, R. Moyer, and J. Watkins, "Loss of energetic beam ions during TAE instabilities," Nuclear Fusion **33**, 749–765 (1993).

[10]S. Cauffman, R. Majeski, K. McClements, and R. Dendy, "Alfvenic behaviour of alpha particle driven ion cyclotron emission in TFTR," Nuclear Fusion **35**, 1597–1602 (1995).

[11]M. Ichimura, H. Higaki, S. Kakimoto, Y. Yamaguchi, K. Nemoto, M. Katano, M. Ishikawa, S. Moriyama, and T. Suzuki, "Observation of spontaneously excited waves in the ion cyclotron frequency range on JT-60U," Nuclear Fusion **48**, 035012 (2008).

[12]K. Saito, R. Kumazawa, T. Seki, H. Kasahara, G. Nomura, F. Shimpo, H. Igami, M. Isobe, K. Ogawa, K. Toi, M. Osakabe, M. Nishiura, T. Watanabe, S. Yamamoto, M. Ichimura, and T. Mutoh, "Measurement of ion cyclotron emissions by using high-frequency magnetic probes in the LHD," Plasma Science and Technology **15**, 209–212 (2013).

[13]S. G. Thatipamula, G. S. Yun, J. Leem, H. K. Park, K. W. Kim, T. Akiyama, and S. G. Lee, "Dynamic spectra of radio frequency bursts associated with edge-localized modes," Plasma Physics and Controlled Fusion **58**, 065003 (2016).

[14]R. Ochoukov, V. Bobkov, B. Chapman, R. Dendy, M. Dunne, H. Faugel, M. Garca-Muoz, B. Geiger, P. Hennequin, K. G. McClements, D. Moseev, S. Nielsen, J. Rasmussen, P. Schneider, M. Weiland, and J.-M. Noterdaeme, "Observations of core ion cyclotron emission on asdex upgrade toka- mak," Review of Scientific Instruments **89**, 10J101 (2018), https://doi.org/10.1063/1.5035180.

[15]L. Askinazi, A. Belokurov, D. Gin, V. Kornev, S. Lebedev, A. Shevelev, A. Tukachinsky, and N. Zhubr, "Ion cyclotron emission in NBI-heated plasmas in the TUMAN-3m tokamak," Nuclear Fusion **58**, 082003 (2018).

[16]E. D. Fredrickson, N. N. Gorelenkov, R. E. Bell, A. Diallo, B. P. LeBlanc, and M. Podest, "Emission in the ion cyclotron range of frequencies (ice) on nstx and nstx-u," Physics of Plasmas **26**, 032111 (2019), https://doi.org/10.1063/1.5081047.

[17]K. Thome, D. Pace, R. Pinsker, M. V. Zeeland, W. Heidbrink, and M. Austin, "Central ion cyclotron emission in the DIII-d tokamak," Nuclear Fusion **59**, 086011 (2019).

[18]N. N. Gorelenkov, "Energetic particle-driven compressional alfvén eigenmodes and prospects for ion cyclotron emission studies in fusion plasmas," New Journal of Physics **18**, 105010 (2016).

[19]F. von Zernike, "Beugungstheorie des schneidenver-fahrens und seiner verbesserten form, der phasenkontrastmethode," Physica **1**, 689–704 (1934).

[20]H. M. Presby and D. Finkelstein, "Plasma phasography," Review of Scientific Instruments **38**, 1563–1572 (1967), https://doi.org/10.1063/1.1720602.

21. H. Weisen, Rev. Sci. Instrum. **59**, 1954 (1988).

22. E. Nelson-Melby, M. Porkolab, P. T. Bonoli, Y. Lin, A. Mazurenko and S.J. Wukitch, Phys. Rev. Lett. **90,** 155004 (2003).

23.N.Tsujii, M. Porkolab, P. T. Bonoli, E. M. Edlund, P. C. Ennever, Y. Lin, J. C. Wright, S. J. Wukitch, E. F. Jaeger, D. L. Green, and R. W. Harvey, "Validation of full-wave simulations for mode conversion of waves in the ion cy- clotron range of frequencies with phase contrast imaging in alcator c-mod," Physics of Plasmas **22**, 082502 (2015), https://doi.org/10.1063/1.4927912.

[24]A. Marinoni, C. P. Moeller, M. Porkolab, J. C. Rost, E. M. Davis, and E. M. Edlund, "A wide frequency heterodyne detection method using the pockels effect," Tech. Rep. (2018).

[25]T. A. Maldonado, "Electro-optic devices," in *The Optics Encyclopedia* (American Cancer Society, 2007) Chap. 13, https://onlinelibrary.wiley.com/doi/pdf/10.1002/9783527600441.oe017.